

# DIGITAL REACTION-DIFFUSION SYSTEM AND ITS APPLICATION

Koichi Ito, Takafumi Aoki and Tatsuo Higuchi

*Graduate School of Information Sciences, Tohoku University  
Aoba-yama 05, Sendai, 980-8579 JAPAN  
ito@higuchi.ecei.tohoku.ac.jp*

**Abstract**— This paper presents a digital reaction-diffusion system (DRDS) – a model of a discrete-time discrete-space reaction-diffusion dynamical system – for designing new image processing algorithms inspired by biological pattern formation phenomena. The original idea is based on the Turing’s model of pattern formation that is widely known in mathematical biology. We first give the definition of DRDS as a discretized reaction-diffusion system. We also present an application of DRDS to fingerprint image restoration.

## I. INTRODUCTION

Living organisms can create a remarkable variety of patterns and forms from genetic information. In embryology, the development of patterns and forms is sometimes called “*Morphogenesis*”. In 1952, Alan Turing suggested that a system of chemical substances, called morphogens, reacting together and diffusing through a tissue, is adequate to account for the main phenomena of morphogenesis [1]. Recently, model-based studies of morphogenesis employing computer simulations have begun to attract much attention in mathematical biology. From an engineering point of view, the insights into morphogenesis provide important concepts for devising a new class of intelligent signal processing algorithms employing biological pattern formation capability. Motivated by this viewpoint, several examples of signal processing algorithms employing Turing’s system have been proposed [2]–[4].

In general, most of computational models of biological pattern formation are described by continuous-time continuous-space reaction-diffusion equations, and hence can not be directly handled by the theory of digital signal processing. Addressing this problem, we propose a *Digital Reaction-Diffusion System* (DRDS) — a model of a discrete-time discrete-space reaction-diffusion dynamical system, which is useful for designing new types of signal processing algorithms based on biological pattern formation mechanism [5]. Using the DRDS, mathematical models of morphogenesis can be understood by multidimensional digital signal processing theory. In this paper, we present the basic

framework of DRDS, and its application to fingerprint image restoration.

## II. DIGITAL REACTION-DIFFUSION SYSTEM

This section defines a digital reaction-diffusion system (DRDS) – a model of a discrete-time discrete-space reaction-diffusion dynamical system having nonlinear reaction kinetics. The general  $M$ -morphogen reaction-diffusion system with two-dimensional (2-D) space indices  $(r_1, r_2)$  is written as

$$\frac{\partial \tilde{\mathbf{x}}(t, r_1, r_2)}{\partial t} = \tilde{\mathbf{R}}(\tilde{\mathbf{x}}(t, r_1, r_2)) + \tilde{\mathbf{D}} \nabla^2 \tilde{\mathbf{x}}(t, r_1, r_2), \quad (1)$$

where

$$\begin{aligned} \tilde{\mathbf{x}} &= [\tilde{x}_1, \tilde{x}_2, \dots, \tilde{x}_M]^T, \\ \tilde{x}_i &: \text{concentration of the } i\text{-th morphogen,} \\ \tilde{\mathbf{R}}(\tilde{\mathbf{x}}) &= [\tilde{R}_1(\tilde{\mathbf{x}}), \tilde{R}_2(\tilde{\mathbf{x}}), \dots, \tilde{R}_M(\tilde{\mathbf{x}})]^T, \\ \tilde{R}_i(\tilde{\mathbf{x}}) &: \text{reaction kinetics for the } i\text{-th morphogen,} \\ \tilde{\mathbf{D}} &= \text{diag}[\tilde{D}_1, \tilde{D}_2, \dots, \tilde{D}_M], \\ \text{diag} &: \text{diagonal matrix,} \\ \tilde{D}_i &: \text{diffusion coefficient of the } i\text{-th morphogen.} \end{aligned}$$

We now sample a continuous variable  $\tilde{\mathbf{x}}$  in (1) at the time sampling interval  $T_0$ , and at the space sampling intervals  $T_1$  and  $T_2$ . Assuming discrete time-index to be given by  $n_0$  and discrete space indices to be given by  $(n_1, n_2)$ , we have

$$\mathbf{x}(n_0, n_1, n_2) = \tilde{\mathbf{x}}(n_0 T_0, n_1 T_1, n_2 T_2). \quad (2)$$

The general DRDS can be written as

$$\begin{aligned} \mathbf{x}(n_0 + 1, n_1, n_2) &= \mathbf{x}(n_0, n_1, n_2) + \mathbf{R}(\mathbf{x}(n_0, n_1, n_2)) \\ &\quad + \mathbf{D}(l * \mathbf{x})(n_0, n_1, n_2), \end{aligned} \quad (3)$$

where

$$\begin{aligned} \mathbf{R} &= T_0 \tilde{\mathbf{R}} = [R_1(\mathbf{x}), R_2(\mathbf{x}), \dots, R_M(\mathbf{x})]^T, \\ \mathbf{D} &= T_0 \tilde{\mathbf{D}} = \text{diag}[D_1, D_2, \dots, D_M], \end{aligned}$$

$$l(n_1, n_2) = \begin{cases} \frac{1}{T_1^2} & (n_1, n_2) = (-1, 0), (1, 0) \\ \frac{1}{T_2^2} & (n_1, n_2) = (0, -1), (0, 1) \\ -2(\frac{1}{T_1^2} + \frac{1}{T_2^2}) & (n_1, n_2) = (0, 0) \\ 0 & \text{otherwise,} \end{cases}$$

and  $*$  is the spatial convolution operator defined as

$$(l * \mathbf{x})(n_0, n_1, n_2) = \begin{bmatrix} (l * x_1)(n_0, n_1, n_2) \\ (l * x_2)(n_0, n_1, n_2) \\ \vdots \\ (l * x_M)(n_0, n_1, n_2) \end{bmatrix}$$

$$= \begin{bmatrix} \sum_{p_1=-1}^1 \sum_{p_2=-1}^1 l(p_1, p_2) x_1(n_0, n_1 - p_1, n_2 - p_2) \\ \sum_{p_1=-1}^1 \sum_{p_2=-1}^1 l(p_1, p_2) x_2(n_0, n_1 - p_1, n_2 - p_2) \\ \vdots \\ \sum_{p_1=-1}^1 \sum_{p_2=-1}^1 l(p_1, p_2) x_M(n_0, n_1 - p_1, n_2 - p_2) \end{bmatrix}.$$

In this paper, we use the two-morphogen DRDS ( $M = 2$ ) with the Brusselator reaction kinetics, which is one of the most widely studied chemical oscillator. The Brusselator-based reaction kinetics for DRDS is defined as

$$\mathbf{R}(\mathbf{x}) = T_0 \begin{bmatrix} k_1 - (k_2 + 1)x_1 + x_1^2 x_2 \\ k_2 x_1 - x_1^2 x_2 \end{bmatrix}. \quad (4)$$

In this paper, we employ the parameter set:  $k_1 = 2$ ,  $k_2 = 4$ ,  $T_0 = 0.01$ ,  $D_1 = 0.01$  and  $D_2 = 0.05$ .

### III. ADAPTIVE DRDS FOR FINGERPRINT RESTORATION

The DRDS with spatially isotropic diffusion terms has produced some broken lines in processing fingerprint images, since it does not take account of the local orientation of ridge flow [5]. In order to solve this problem, this section presents an adaptive DRDS model, in which we can use the local orientation of the ridge in the fingerprint image to guide the action of DRDS. This can be realized by introducing orientation masks to be convolved with the diffusion terms. A two-morphogen adaptive DRDS can be written as

$$\begin{aligned} \mathbf{x}(n_0 + 1, n_1, n_2) \\ = \mathbf{x}(n_0, n_1, n_2) + \mathbf{R}(\mathbf{x}(n_0, n_1, n_2)) \\ + \mathbf{D}(\mathbf{h}^{n_1 n_2} * l * \mathbf{x})(n_0, n_1, n_2), \end{aligned} \quad (5)$$

where  $\mathbf{h}^{m_1 m_2}(n_1, n_2) = [h_1^{m_1 m_2}(n_1, n_2), h_2^{m_1 m_2}(n_1, n_2)]^T$ ,  $h_i^{m_1 m_2}(n_1, n_2)$ : orientation mask at the pixel  $(m_1, m_2)$  for the  $i$ -th morphogen,

$$\begin{aligned} (\mathbf{h}^{n_1 n_2} * l * \mathbf{x})(n_0, n_1, n_2) \\ = \begin{bmatrix} (h_1^{n_1 n_2} * l * x_1)(n_0, n_1, n_2) \\ (h_2^{n_1 n_2} * l * x_2)(n_0, n_1, n_2) \end{bmatrix}. \end{aligned}$$

We consider the problem of restoring the original fingerprint images from blurred images by using adaptive DRDS. Let assume that a set of exact orientation masks  $\mathbf{h}^{m_1 m_2}(n_1, n_2)$  have already been obtained. In this case, we can restore fingerprint images as follows. We first store an initial (blurred) fingerprint image in  $x_1(0, n_1, n_2)$ , at time 0. After computing the dynamics for  $n_0$  steps, we obtain the output image (restored fingerprint) from  $x_1(n_0, n_1, n_2)$ . Assume that we use the parameter set for the Brusselator reaction kinetics described in the previous section. The dynamics has the equilibrium  $(x_1, x_2) = (2, 2)$ , and the variation ranges of variables  $(x_1, x_2)$  are bounded around the equilibrium point as  $1 \leq x_1 \leq 3$  and  $1 \leq x_2 \leq 3$ . Hence, we first scale the  $[0, 255]$  gray-scale fingerprint image into  $[1, 3]$  range. The scaled image becomes the initial input  $x_1(0, n_1, n_2)$ , while the initial condition of the 2nd morphogen is given by  $x_2(0, n_1, n_2) = 2$  (equilibrium). The zero-flux Neumann boundary condition is employed for computing the dynamics. After  $n_0$  steps of DRDS computation, we obtain  $x_1(n_0, n_1, n_2)$  as the output image, which is scaled back into the  $[0, 255]$  gray-scale image to produce the final output. Spatial sampling parameters  $T_1$  and  $T_2$  are adjusted according to the inherent spatial frequency of original fingerprints.

In practical situation, it is difficult to obtain exact orientation masks from blurred fingerprint images. Addressing this problem, we employ the hierarchical procedure for adaptive DRDS processing as follows.

1. Partition an input image into 4 sub-images.
2. Generate four different orientation masks for four sub-images, and run the adaptive DRDS for  $n_0 = 10$  steps.
3. Carry out the same process increasing the number of image partitions as 9, 16, 36, 64 and 81.
4. Calculate orientation masks for every pixel, and run the adaptive DRDS until  $n_0 = 500$ .

In the above process, we define the orientation mask  $h_1^{m_1 m_2}(n_1, n_2)$  at the pixel  $(m_1, m_2)$  as a  $32 \times 32$  real coefficient matrix having values within the window  $(n_1, n_2) = (-16, -16) \sim (15, 15)$ , which can be automatically derived as follows (Figure 1): (i) Fourier transform the local image around the pixel  $(m_1, m_2)$  in terms of space indices  $(n_1, n_2)$ , (ii) extract the dominant ridge orientation  $\theta$  from transformed image, (iii) generate the mask pattern  $H_1^{m_1 m_2}(j\omega_1, j\omega_2)$  having the orientation  $\theta$  in frequency domain:

$$H_1^{m_1 m_2}(j\omega_1, j\omega_2) = \begin{cases} 1 & \text{for unstable frequency band} \\ & \text{(black pixels in Figure 1(iii))} \\ 2 & \text{otherwise,} \end{cases}$$

and (iv) taking the inverse Fourier transform to obtain the orientation mask  $h_1^{m_1 m_2}(n_1, n_2)$ . The orientation mask  $h_2^{m_1 m_2}(n_1, n_2)$  for the second morphogen, on the

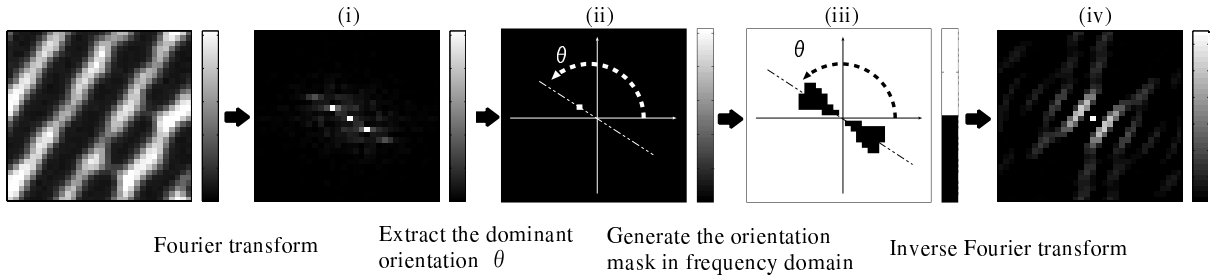


Figure 1: Generation of the orientation mask.

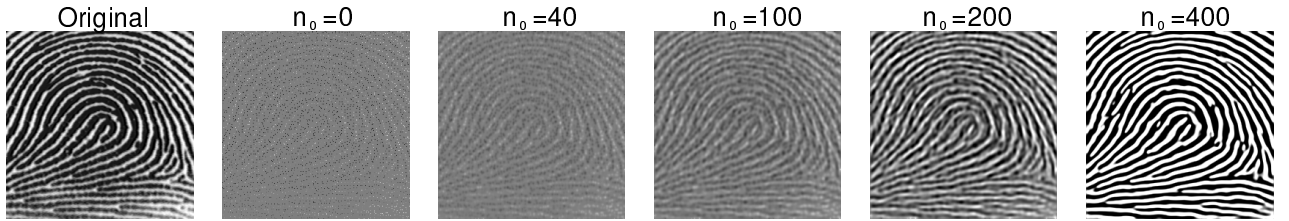


Figure 2: Fingerprint image restoration from  $1/(4 \times 4)$  subsampled image using adaptive DRDS.

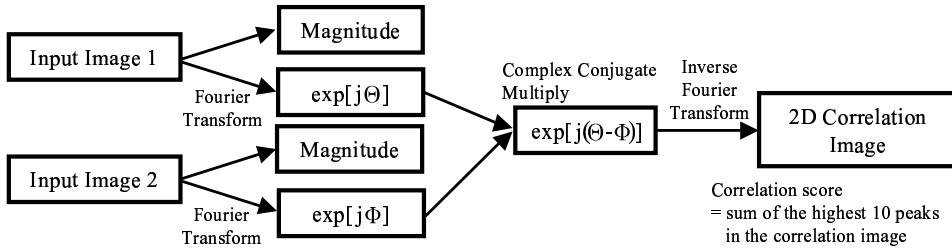


Figure 3: Computation flow of Phase-Only Correlation (POC).

other hand, has the value 1 at the center  $(n_1, n_2) = (0, 0)$ , and equals to 0 for other coordinates  $(n_1, n_2)$ . Thus, the dynamics for the morphogen  $x_2(n_0, n_1, n_2)$  does not take account of the local orientation.

#### IV. EXPERIMENTS AND DISCUSSIONS

In order to evaluate the restoration capability, we apply the adaptive DRDS to the problem of restoring original fingerprints from subsampled fingerprint images. For this purpose, we generate a subsampled fingerprint image from an original fingerprint image as follows: (i) partition the original image into  $R \times S$ -pixel rectangular blocks, and (ii) select one pixel randomly from every block and eliminate all the other pixels (set 127 to the pixels). The image thus obtained has the same size as the original image, but the number of effective pixels is reduced to  $1/(R \times S)$ . We use subsampled images as input to adaptive DRDS. For example, Figure 2 shows the restoration of a fingerprint image from  $1/(4 \times 4)$  subsampled image.

The restoration capability of adaptive DRDS is evaluated by calculating the similarity between the o-

iginal fingerprint image and the restored image. As a measure of similarity, we employ Phase-Only Correlation (POC), which has an efficient discrimination capability for fingerprint identification [6]. Figure 3 shows the computation flow of POC. In our experiment, we use ten fingerprint images (Sample01–Sample10) with subsampling rates  $1/(4 \times 4)$  and  $1/(5 \times 5)$ . Figure 4 shows the variation of correlation scores between the original fingerprint image of Sample01 and the 10 images restored from  $1/(4 \times 4)$  subsampled images of Sample01–Sample10. We can confirm that the similarity between the original Sample01 and the corresponding restored image increases as the number of steps  $n_0$  increases. The optimal discrimination capability could be obtained around  $n_0 = 400$ . In the range of  $n_0 = 200 \sim 300$ , the correlation scores for the wrong fingerprints drop steeply while the correct fingerprint keeps sufficient level of correlation.

Tables 1 and 2 summarize correlation scores (at  $n_0 = 400$ ) between original and restored images of Sample01–Sample10 for subsampling rates  $1/(4 \times 4)$  and  $1/(5 \times 5)$ , respectively. For both cases, auto-

Table 1: Correlation scores at  $n_0 = 400$  (restoration from  $1/(4 \times 4)$  subsampled images)

		Restored Image									
		Sample01	Sample02	Sample03	Sample04	Sample05	Sample06	Sample07	Sample08	Sample09	Sample10
Original Image	Sample01	0.718	0.232	0.337	0.361	0.323	0.334	0.260	0.232	0.350	0.267
	Sample02	0.350	0.673	0.382	0.380	0.298	0.331	0.302	0.248	0.270	0.247
	Sample03	0.334	0.253	0.829	0.361	0.333	0.324	0.309	0.275	0.269	0.263
	Sample04	0.319	0.271	0.386	0.758	0.289	0.286	0.329	0.245	0.267	0.258
	Sample05	0.343	0.245	0.351	0.362	0.699	0.285	0.350	0.245	0.289	0.262
	Sample06	0.320	0.264	0.299	0.365	0.321	0.670	0.285	0.247	0.272	0.257
	Sample07	0.298	0.233	0.383	0.341	0.319	0.323	0.683	0.244	0.280	0.254
	Sample08	0.286	0.239	0.305	0.310	0.283	0.273	0.246	0.581	0.258	0.244
	Sample09	0.319	0.251	0.331	0.308	0.280	0.280	0.269	0.239	0.614	0.282
	Sample10	0.242	0.219	0.273	0.306	0.281	0.262	0.242	0.204	0.285	0.637

Table 2: Correlation scores at  $n_0 = 400$  (restoration from  $1/(5 \times 5)$  subsampled images)

		Restored Image									
		Sample01	Sample02	Sample03	Sample04	Sample05	Sample06	Sample07	Sample08	Sample09	Sample10
Original Image	Sample01	0.684	0.224	0.318	0.325	0.272	0.261	0.283	0.247	0.311	0.245
	Sample02	0.336	0.563	0.339	0.337	0.252	0.262	0.298	0.225	0.278	0.236
	Sample03	0.303	0.262	0.748	0.340	0.273	0.323	0.333	0.260	0.281	0.251
	Sample04	0.324	0.234	0.366	0.582	0.293	0.313	0.332	0.235	0.284	0.249
	Sample05	0.322	0.221	0.292	0.394	0.534	0.298	0.352	0.249	0.317	0.262
	Sample06	0.340	0.252	0.337	0.390	0.276	0.551	0.289	0.282	0.286	0.248
	Sample07	0.279	0.234	0.356	0.294	0.275	0.256	0.607	0.222	0.271	0.258
	Sample08	0.282	0.206	0.303	0.267	0.230	0.270	0.269	0.546	0.242	0.246
	Sample09	0.287	0.224	0.335	0.312	0.244	0.254	0.298	0.260	0.573	0.250
	Sample10	0.254	0.207	0.302	0.319	0.222	0.246	0.249	0.229	0.238	0.529

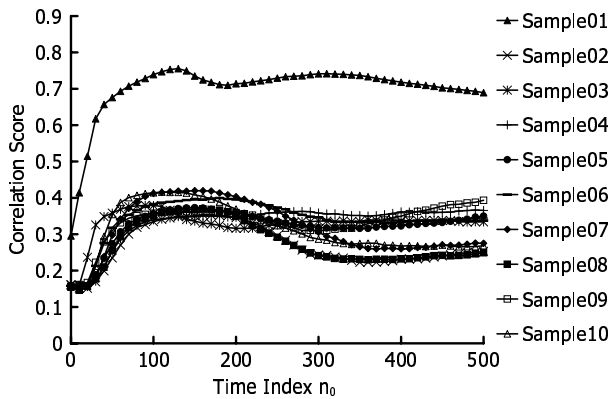


Figure 4: Correlation scores between the original image of Sample01 and the restored images of Sample01–Sample10 (restoration from  $1/(4 \times 4)$  subsampled images).

correlation exhibits significantly higher scores than the cross-correlation scores. These examples demonstrate a potential capability of adaptive DRDS to enhance the performance of matching algorithms for blurred fingerprint images.

## V. CONCLUSION

This paper presents a digital reaction-diffusion system (DRDS) – a model of a discrete-time discrete-space reaction-diffusion dynamical system – useful for signal processing and computer graphics applications. This

paper also describes the design of an adaptive DRDS having the capability to reconstruct a complete fingerprint pattern from a blurred image. We are expecting that the framework of DRDS may provide a theoretical foundation of *digital morphogenesis*, that is, a technique for applying the principle of biological pattern formation phenomena to many engineering problems.

## References

- [1] A. M. Turing, “The chemical basis of morphogenesis,” *Phil. Trans. R. Soc. London*, Vol. B237, pp. 37–72, Aug. 1952.
- [2] K. R. Crounse and L. O. Chua, “Methods for image processing and pattern formation in cellular neural networks: a tutorial,” *IEEE Trans. Circuits Syst.-I*, Vol. 42, No. 10, pp.583–601, Oct. 1995.
- [3] L. Goras, L. O. Chua and L. Pivka, “Turing patterns in CNNs–part II: equations and behaviors,” *IEEE Trans. Circuits Syst.-I*, Vol. 42, No. 10, pp.612–626, Oct. 1995.
- [4] A. S. Sherstinsky and R. W. Picard, “M-lattice: from morphogenesis to image processing,” *IEEE Trans. Image Processing*, Vol. 5, No. 7, pp. 1137–1150, July 1996.
- [5] K. Ito, T. Aoki, and T. Higuchi, “Digital reaction-diffusion system – A foundation of bio-inspired texture image processing,” *IEICE Trans. Fundamentals*, Vol. E84-A, No. 8, pp. 1909–1918, Aug. 2001.
- [6] K. Kobayashi, H. Nakajima, T. Aoki, M. Kawamata and T. Higuchi, “Principles of phase only correlation and its applications,” (in Japanese), *ITE Technical Report*, Vol.20, No.41, pp.1–6, July 1996.